

ANALYSIS OF CIRCULARLY POLARIZED RING SLOT ANTENNA FED BY COUPLING STRIP WITH RESISTIVE LOADING

C.-C. Wang¹ and J.-S. Row^{2,*}

¹Department of Information Technology, Kao Yuan University, Kaohsiung 821, Taiwan, R.O.C.

²Department of Electrical Engineering, National Changhua University of Education, Chang-Hua 500, Taiwan, R.O.C

Abstract—An analysis for circularly-polarized (CP) ring slot antennas fed by a coupling strip with resistive loading is presented. By treating the antenna as a two-port circuit, the amplitudes and phases of two orthogonal modes excited from the slot antenna can be found and expressed in terms of the S parameters of the circuit. The axial ratio calculated through the S parameters has a good agreement with that obtained from the pattern simulation of IE3D. The effects of varying key parameters of the coupling strip on the amplitudes and phases of the dual orthogonal modes are investigated in detail.

1. INTRODUCTION

For a single-fed resonant antenna, the design process for circular polarization (CP) is more tedious than that for linearly polarization. The main reason is that the parameters related to CP axial ratio need to be exactly determined, especially for the resonant antennas with a high quality factor. Take a CP patch antenna realized with perturbation technologies [1–9] as an example, the dimensions of the perturbation segments have to be fine-tuned in the design stage, and after each tuning, the antenna radiation characteristics need to be simulated afresh until the minimum axial ratio is found. This is a cut-and-try and time-consuming process. Recently, we have demonstrated that the CP radiation can be naturally generated from a ring slot antenna excited by an L-shaped coupling strip with resistive loading [10]. The advantage of the feed mechanism

Received 26 April 2012, Accepted 11 June 2012, Scheduled 16 June 2012
* Corresponding author: Jeen-Sheen Row (jsrow@cc.ncue.edu.tw).

is that the axial ratio is not very sensitive to the variations of the loading-resistance value and the coupling-strip width, which are the parameters dominating the CP performances; besides, the antenna gain is not obviously degraded as long as the loading resistance is small enough. On the other hand, the antenna itself can also take the place of the loading resistor, and with successive iteration, a series-feed CP slot array can be built. In this paper, a simple analysis for the CP operation of the ring slot antenna is given. Due to the existence of the loading resistance, the antenna is treated as a two-port circuit. For two orthogonal modes forming the CP radiation, the amplitude ratio and phase difference between them at the CP operating frequency can be respectively derived from the S parameters of the circuit. It represents that the CP axial ratios of the cases with various loading-resistance values can be directly calculated with the S parameters, and consequently the EM simulation to the antenna radiation characteristics is not necessary in the design stage.

2. ANTENNA CONFIGURATION

Figure 1 shows the studied antenna structure which is the same as that in [10]. The slot antenna is operated at the frequency whose wavelength in the slot approximately corresponds to the mean circumference of the ring slot. With the coupling strip, two fundamental modes of the slot antenna can be excited in series. Because the exciting amplitudes and phases of the two modes only depend on the field distributions along the coupling strip, it is reasonable to assume that the CP

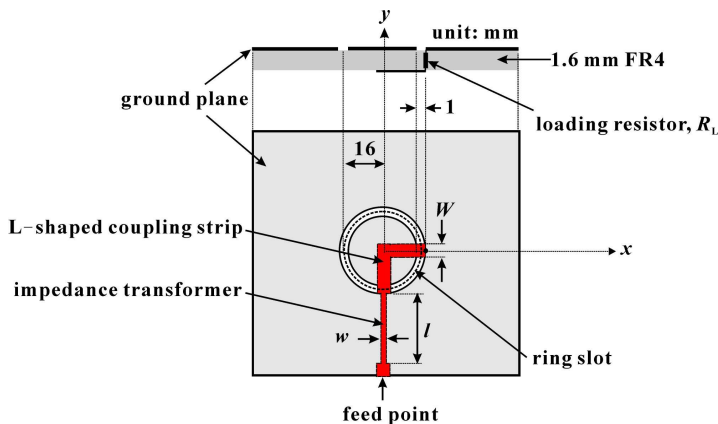


Figure 1. Geometry of the studied antenna.

axial ratio is related to (W, R_L) and nearly has nothing to do with (l, w) . Therefore, the impedance transformer is excluded from the antenna for the analysis to the CP axial ratio, and the remainder structure can be treated as a two-port reciprocal network, in which Port 1 and Port 2 are respectively set at the two edges of the coupling strip. Once the optimum axial ratio is found, concurrent with the corresponding CP frequency and impedance, the dimensions of the impedance transformer can be easily determined.

3. CP AXIAL RATIO CALCULATED FROM S PARAMETERS

The schematic diagram for the studied case and its equivalent two-port network are given in Fig. 2. The far-field pattern of the slot antenna is due to the radiations of the two orthogonal modes, M_x and M_y , excited by the coupling strip, and their feed points, the intersections of the slot and the coupling line, have a separated distance of a quarter wavelength along the slot circumference. This suggests that the maximums or minimums of the field distributions of the two modes are located at the two feed points as the slot antenna is resonant. Consequently, the excitations of the two modes can be totally treated as the form of magnetic coupling or electric coupling. In regard to the magnetic coupling, the coupling factor from the feed line to the slot is related to the magnetic field, produced by the currents flowing on the feed line, within their intersections [11, 12]. Provided that d is small, the magnitudes of the magnetic fields at the under and right intersections can be regarded as constants, and they can be equivalent to the amplitudes of the electric currents I_1 and I_2 , respectively. Therefore, the magnitude of I_1/I_2 represents the amplitude ratio of M_y mode to M_x mode. As for the phase difference between the two modes, it can

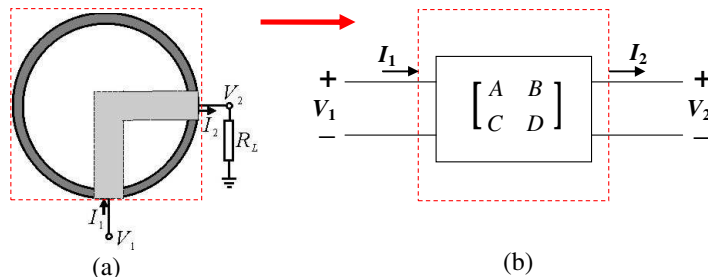


Figure 2. (a) Schematic diagram for the studied antenna. (b) Equivalent two-port network.

be found by evaluating the argument of $-V_1/V_2$ because V_1 (for M_y mode) and $-V_2$ (for M_x mode) are set at the symmetrical positions with respect to the ring slot. To derive the expressions of I_1/I_2 and $-V_1/V_2$, the two-port network is described with the $ABCD$ matrix. According to the definition, the voltages and currents at Port 1 and Port 2 have the following relations

$$V_1 = AV_2 + BI_2 \quad (1)$$

$$I_1 = CV_2 + DI_2 \quad (2)$$

Dividing Eqs. (1) and (2) by V_2 and I_2 , respectively, gives

$$\frac{V_1}{V_2} = A + B \frac{I_2}{V_2} = A + \frac{B}{R_L} \quad (3)$$

$$\frac{I_1}{I_2} = C \frac{V_2}{I_2} + D = CR_L + D \quad (4)$$

where the ratio of V_2 to I_2 has to satisfy the boundary condition, that is, the loading resistance R_L . With the conversion from $ABCD$ parameters to S parameters [12], the amplitude ratio (K) and the phase difference (δ) between M_y and M_x modes can be expressed as

$$K = \left| \frac{M_y}{M_x} \right| = \left| \frac{I_1}{I_2} \right| = \left| \frac{R_L (1 - S_{11})^2 - S_{21}^2}{Z_0} + \frac{(1 - S_{11})(1 + S_{11}) + S_{21}^2}{2S_{21}} \right| \quad (5)$$

$$\delta = \angle M_y - \angle M_x = \angle V_1 - \angle -V_2 \\ = \arg \left[-\frac{(1 + S_{11})(1 - S_{11}) + S_{21}^2}{2S_{21}} - \frac{Z_0 (1 + S_{11})^2 - S_{21}^2}{R_L 2S_{21}} \right] \quad (6)$$

where the identities of $S_{12} = S_{21}$ and $S_{22} = S_{11}$ have been used. Once K and δ are acquired, the CP axial ratio of the slot antenna can be determined by [13]

$$AR_{\text{dB}} = 20 \log |\cot \varepsilon|, \quad \varepsilon = \frac{1}{2} \sin^{-1} (\sin 2\gamma \cdot \sin \delta) \quad (7)$$

in which $\gamma = \tan^{-1} K$.

4. PARAMETER ANALYSES

The example with $W = 5$ mm and $R_L = 50\Omega$ is first selected to confirm the validity of the axial ratio calculated from S parameters. To obtain the required S parameters from IE3D, the example antenna is simulated by setting Port 1 and Port 2 at the two edges of the coupling strip, in which Port 1 is a source port and Port 2 is a loading port with pure resistance R_L . It has to be mentioned that the axial ratio of such a two-port antenna circuit can also be obtained directly

from the radiation pattern simulation of IE3D, but the whole antenna structure has to be simulated afresh once R_L is changed. For the example antenna, the frequency response of the axial ratio calculated from the S parameters is presented in Fig. 3 along with the results obtained from the pattern simulation. They have good agreements around the frequencies with the minimum axial ratios; however, an obvious difference between them is observed off the CP operating frequency. One of the reasons is that the axial ratio calculated from the S parameters is based on the assumption that the field in the slot has the distribution mode of one wavelength at any frequency, but the axial-ratio results obtained from the pattern simulation include the effects of the variations of the field distributions against frequency.

Figure 3 also shows the results for the cases of various W values. The achievable minimum axial ratios (AAR_{min}) for the cases of $W = 1, 5$, and 10 mm are $1.9, 0.5$, and 1.5 dB, respectively; in addition, their corresponding frequencies, named CP center frequency (f_c), are $2.31, 2.45$, and 2.62 GHz. For the three cases, their K and δ values are also calculated using Eqs. (5) and (6), and the results are exhibited in Fig. 4. It is found that at their respective CP center frequencies, the three cases have almost the same K value (about 1.1) but obviously different δ values. The δ value is 89° for the $W = 5$ mm case, giving a nearly perfect CP radiation; however, it is reduced to 78° for the $W = 1$ mm case, leading to an increase of about 1.4 dB in AAR_{min} .

When the other dimensions are the same as those of the example antenna, the effects of varying R_L on AAR_{min} and f_c are presented in Fig. 5. From the results, it is confirmed that the proposed axial-ratio calculation method can offer an acceptable prediction on AAR_{min} and f_c even for the coupling strip loaded with different R_L . The variations of K and δ at the CP center frequency against R_L are also shown

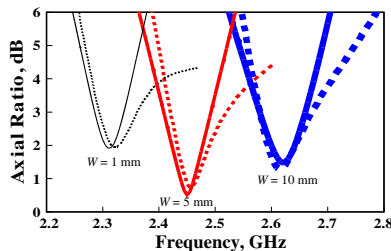


Figure 3. Simulated (solid line) and calculated (broken line) axial ratio results for the example antenna with various W .

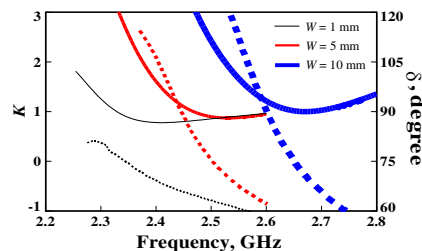


Figure 4. Variations of K (solid line) and δ (broken line) against frequency for the example antenna with various W .

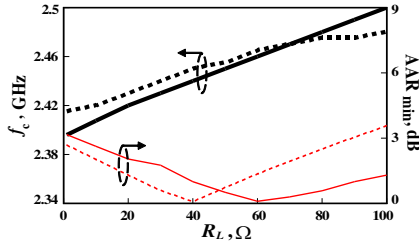


Figure 5. Simulated (solid line) and calculated (broken line) CP performances for the example antenna with various R_L .

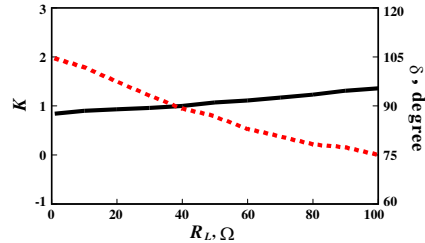


Figure 6. Variations of K (solid line) and δ (dashed line) against R_L .

in Fig. 6. The results demonstrate that with increasing R_L , the K value is increased from 0.86 to 1.36 and the δ value is decreased from 105° to 75°. As a consequence, the cases of $R_L = 1$ and 100Ω have worse CP performances, whose AAR_{min} values, calculated from the S parameters, are 2.7 and 3.6 dB, respectively. According to the previous analysis to W , the coupling strip with a narrower width has a smaller phase difference at the CP center frequency, which suggests that the CP performance of the $R_L = 1\Omega$ case can be improved by reducing its phase difference through narrowing the coupling strip. However, the CP center frequency has a certain decrease with narrowing the coupling strip, as shown in Fig. 3.

5. EXPERIMENTAL RESULTS

The example antenna with the impedance transformer was first fabricated, and the measured results are given in Fig. 7. It is seen that the minimum axial ratio occurs at 2.46 GHz and its value is about 1.5 dB. In addition to experimental errors, the difference between the measured and simulated results of the example antenna could be due to the value of R_L , which cannot be exactly determined in the experiment. When the loading resistance is changed from 50Ω to 1Ω , the axial ratio is increased to 2.5 dB and the corresponding frequency is reduced to 2.41 GHz. To improve the CP performance, another prototype, using a narrower coupling strip ($W = 3\text{ mm}$), was constructed. The experimental results of the prototype are also shown in Fig. 7, and they clearly demonstrate that the axial ratio is lowered to 0.6 dB as expectation. In addition, its CP center frequency has a decrease of 20 MHz as compared to the example antenna with $R_L = 1\Omega$. The prototype has bidirectional radiation patterns with low

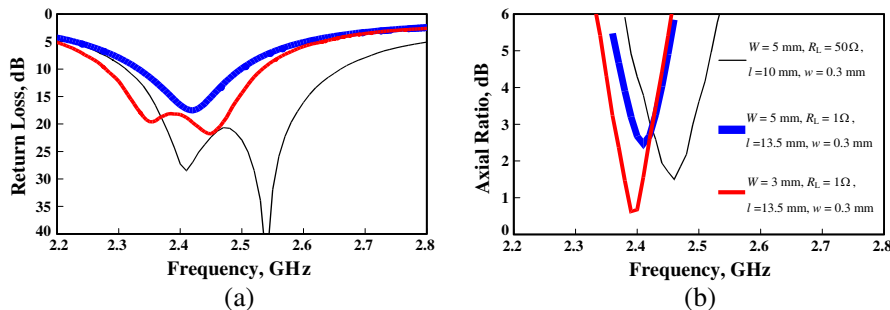


Figure 7. Measured results for the constructed prototypes; the other dimensions are shown in Fig. 1. (a) Return loss. (b) Axial ratio.

cross polarization and the peak gain of around 3.3 dBic. These results have been exhibited in [10].

6. CONCLUSIONS

A simple analysis for the circularly-polarized ring slot antenna excited with an L-shaped coupling strip with resistive loading has been presented. By treating the antenna as a two-port circuit, the amplitude ratio and phase difference of two orthogonal modes forming the circular polarization radiation can be derived using the *S* parameters of the circuit. In addition, the axial ratio results calculated from the *S* parameters agree well with those acquired from the time-consuming pattern simulation of IE3D, and they are also validated by experiments.

REFERENCES

1. Sharma, P. C. and K. C. Gupta, "Analysis and optimum design of single feed circularly polarized microstrip antennas," *IEEE Trans. on Antennas and Propagat.*, Vol. 31, 949–955, 1983.
2. Kasabegoudar, V. G. and K. J. Vinoy, "A broadband suspended microstrip antenna for circular polarization," *Progress In Electromagnetics Research*, Vol. 90, 353–368, 2009.
3. Bao, X. L. and M. J. Ammann, "Comparison of several novel annular-ring microstrip patch antennas for circular polarization," *Journal of Electromagnetic Waves and Applications*, Vol. 20, No. 11, 1427–1438, 2012.
4. Wu, F.-X., W.-M. Li, and S.-M. Zhang, "Dual-band CPW-fed circularly-polarized slot antenna for DMB/Wimax applications,"

- Progress In Electromagnetics Research Letters*, Vol. 30, 185–193, 2012.
- 5. Liao, W. and Q.-X. Chu, “Dual-band circularly polarized microstrip antenna with small frequency ratio,” *Progress In Electromagnetics Research Letters*, Vol. 15, 145–152, 2010.
 - 6. Deng, J.-Y., Y.-Z. Yin, Y.-H. Huang, J. Ma, and Q.-Z. Liu, “Compact circularly polarized microstrip antenna with wide beamwidth for compass satellite service,” *Progress In Electromagnetics Research Letters*, Vol. 11, 113–118, 2009.
 - 7. Wu, G.-L., W. Mu, G. Zhao, and Y.-C. Jiao, “A novel design of dual circularly polarized antenna fed by L-strip,” *Progress In Electromagnetics Research*, Vol. 79, 39–46, 2008.
 - 8. Han, T.-Y. and C. Y. D. Sim, “Probe-feed circularly polarized square-ring microstrip antennas with thick substrate,” *Journal of Electromagnetic Waves and Applications*, Vol. 21, No. 1, 71–80, 2007.
 - 9. Liu, W.-C. and P.-C. Kao, “Design of a probe-fed H-shaped microstrip antenna for circular polarization,” *Journal of Electromagnetic Waves and Applications*, Vol. 21, No. 7, 857–864, 2007.
 - 10. Wang, C. C., T. Y. Lee, and J. S. Row, “A simple design for circularly polarized ring-slot antennas,” *Microwave Opt. Technol. Lett.*, Vol. 53, 2263–2265, 2011.
 - 11. Pozar, D. M., “Microstrip antenna aperture-coupled to a microstripline,” *Electron. Lett.*, Vol. 21, 49–50, 1985.
 - 12. Pozar, D. M., *Microwave Engineering*, Wesley, New York, 1998.
 - 13. Kraus, J. D., *Antennas*, McGraw-Hill, New York, 2002.